Scientific Research Publishing

New Journal of Glass and Ceramics, 2018, 8, 12-21
http://www.scirp.org/journal/njgc
ISSN Online: 2161-7562
ISSN Print: 2161-7554

More Insight on Structure of New Binary Cerium Borate Glasses

Gomaa El-Damrawi[1], Fawzeya Gharghar[1], Rawya Ramadan[2]

[1]Glass Research Group, Physics Department, Faculty of Science, Mansoura University, Mansoura, Egypt
[2]Microwave and Dielectric Department, Physics Division, National Research Centre, Giza, Egypt
Email: gomaaeldamrawi@gmail.com

How to cite this paper: El-Damrawi, G., Gharghar, F. and Ramadan, R. (2018) More Insight on Structure of New Binary Cerium Borate Glasses. *New Journal of Glass and Ceramics*, **8**, 12-21.
https://doi.org/10.4236/njgc.2018.81002

Received: December 7, 2017
Accepted: January 26, 2018
Published: January 29, 2018

Abstract

The structure of glasses in the system of $xCeO_2(100 - x)B_2O_3$, x = 30, 40, 50 mol% CeO_2 has been explored for the first time by correlation between data obtained from XRD, FTIR and ^{11}B NMR analyses. NMR spectroscopy and FTIR spectroscopy have confirmed that transformation rate of BO_3 to BO_4 groups is reduced by CeO_2 addition. The concentration of Ce_4-O-Ce_4 is increased at the expense of both B_4-O-Ce_4 and B_3-O-B_4 linkages. Boron atoms are mainly coordinated with Ce_4 sites as second neighbors due to increasing CeO_4 species with further increase of CeO_2 concentration. Increasing B_4 fraction is considered due to forming of CeO_4 with rate higher than that of BO_4 units. The change of chemical shift of ^{11}B nuclei upon exchanging B_2O_3 with CeO_2 confirms that the central boron atoms would be coordinated with tetrahedral cerium atoms as second neighbors. The X-ray diffraction of cerium rich glass is clearly indicated that the formation of crystalline phases refers to CeO_4, $CeBO_3$ and $Ce(BO_2)_3$ species.

Keywords

Borate, Cerium, Former Units, NMR Analysis

1. Introduction

Borate glasses have attracted a great interest [1] [2] [3] [4] due to their desirable properties such as low melting temperature, high transparency, and good thermal stability. In addition, these glasses are promising host network to incorporate high concentrations from rare earth elements such as CeO_2 [5]-[12]. The great importance of cerium ions is known [13]-[19] to come from their interesting characteristics such as physical, optical, catalytic and as well as magnetic properties. Particular technological applications including gamma ray shielding,

luminescent, scintillators and dielectric, optical and electronic device are highly related to structural role of CeO_2 in glasses.

Addition of a network modifier to B_2O_3 is reported [20] [21] [22] [23] [24] to break the B-O bonds and induce the transformation of BO_3 triangles to BO_4 tetrahedral units. On the other hand, CeO_2 plays different role when it is added to B_2O_3 since CeO_2 enters to the glass network as an intermediate oxide. The modification part of CeO_2 produces the conversion from BO_3 to BO_4 groups while the rest of CeO_2 can participate in the glass network to form CeO_4 tetrahedral groups.

In this regard, few structural studies on binary cerium borate glasses have been done [5] [9] [12] [25]. Changing in cerium environment around boron central atoms explains the dominant role of cerium oxide when it enters to the glass matrix as a glass former. Cerium thus behaves more as a glass modifier in low cerium content and plays the dual role at higher CeO_2 concentration.

It is aimed in the present study to determine the structural role of CeO_2 in cerium rich glasses by using the advantage of NMR spectroscopy, since to our knowledge, no studies in this regard have been carried out.

2. Experimental Details

2.1. Sample Preparation

The glass samples have been prepared by the normal melting method using cerium oxide (CeO_2) and boric oxide (H_3BO_3) as starting materials. The appropriate amount of high purity chemical compounds were well mixed together to obtain fine powder. The batch mixture was then transferred to an alumina crucible and fused in an electric furnace. The melting process was carried out at different temperatures ranging between 900˚C and 1450˚C depending on the glass compositions. The melt was stirred several times until a complete homogenization was obtained. Each melt was then poured on stainless steel plate and pressed by another plate to take the final shape.

2.2. Measurement Tools

2.2.1. X-Ray Diffraction (XRD)

XRD measurements were carried out on powdered samples at (Metallurgical Institute, El-Tebbeen-Helwan) using a BrukerAxs-D8 Advance powder XRD system with a Cu Kα radiation ($\lambda_{CuK\alpha}$ = 0.1540600 nm).

The range of the diffraction angle (2θ) is changed from 4˚ to 70˚ using a dwell time of 0.4 seconds.

2.2.2. ^{11}B NMR Measurements

Solid-state ^{11}B NMR spectra were performed at Magnetic Resonance unit, Mansura University. The samples were measured with JEOL GSX-500 high-resolution solid-state MAS NMR spectrometer in a magnetic field of 11.74 T at ^{11}B Larmor frequency of 160.4 MHz and spinning rate of 15 KHz. A single pulse length was

used of 0.5 - 1.0 ms with a pulse delay of 2.5 s, and an accumulation of 200 - −300 scans. All Samples were grinded to fine powders then filled into standard 4 mm NMR sample tubes.

2.2.3. Fourier Transform Infrared Spectra (FTIR)

FTIR Spectra of powdered glasses were obtained in the wavenumber range of 400 to 4000 cm^{-1} using a Fourier transform IR spectrometer (Mattson 5000, Fine Measurements Laboratory, Mansura University, Egypt) with a resolution of 2 cm^{-1}. Each sample was mixed with KBr by the ratio 1:100 in weight and then subjected to a pressure of load of 5 tons/cm^2 to produce a homogeneous pellet. The infrared absorbance measurements were carried out at room temperature immediately after preparing.

The spectra were corrected for the background and the dark current noises using two points baseline corrections then were normalized by making the absorption of every spectrum varying from zero to one reported in arbitrary units.

3. Results and Discussion

3.1. X-Ray Analysis

Figure 1 presents XRD diffraction patterns for $xCeO_2(100 - x)B_2O_3$ with x = 30, 40, 50 mol% CeO_2. The compositions of 30 and 40 mol% CeO_2 were mainly amorphous, whereas composition containing 50 mol% CeO_2 was partially crystallized. As it can be a notable, the amorphous structure of the glass network

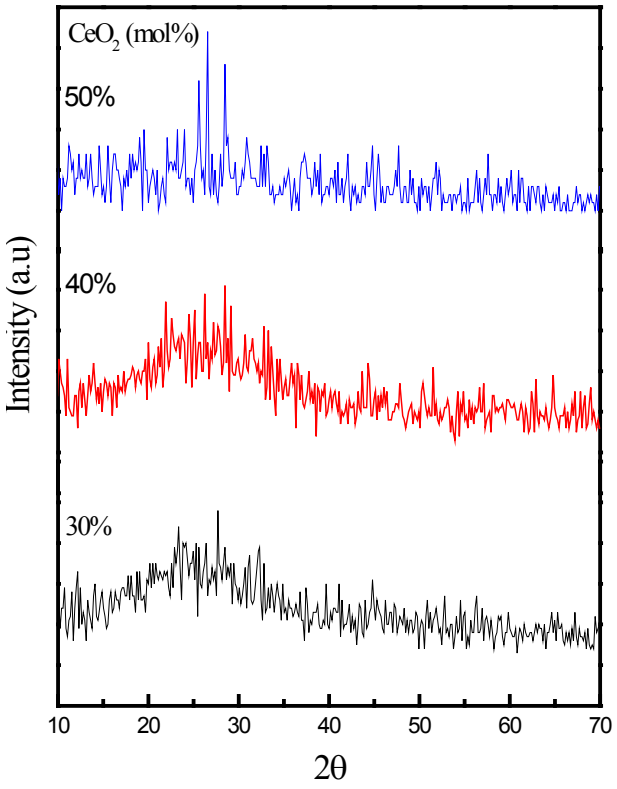

Figure 1. XRD patterns of binary cerium borate a function of CeO_2 concentration.

containing 30 and 40 mol% CeO_2 is clearly evidenced, since a broad hump characterizing this feature is indicated in the XRD spectra of the glasses. On the other hand, sharper XRD peaks are developed on the spectra of glass contains 50 mol% CeO_2. The discrete sharp lines observed at ~25.7, 28.6, 30.8, 37.6, 47.49˚ are mainly assigned to crystalline CeO_4[PDF nr.810792], $CeBO_3$[PDF nr.210177] and $Ce(BO_2)_3$[PDFnr.230877] species. The strong tendency to crystallization may attributed to increasing in network connectivity as result of further concentration of tetrahedral CeO_4 as former species [9] [10] [12]. The tetrahedral CeO_4 groups have the priority to combine together with B atoms and form an ordered structural chain in Ce-O-B linkages causing an increment in crystallization.

These considerations are further supported through comparison between XRD pattern of pure CeO_2 as shown in **Figure 2** and that of cerium borate glass containing 50 mol% CeO_2. Both spectra offer sharp diffraction lines ranged between 25˚ and 35˚. On other hand, the intensities of diffraction patterns of cerium borate glass are appeared to be lower than that of pure CeO_2. In such a case, the distribution of the accumulated CeO_4 units within the amorphous borate structure units may play the role of lowering the crystallinty.

3.2. ^{11}B NMR Spectroscopy

^{11}B NMR spectra of alkali modified borate glasses were generally possessed two well separated peaks [10] [26] [27] [28] [29]. One is corresponding to BO_3 and the other is related to BO_4 sites. The broad ^{11}B NMR resonance with peak centered at about ~12 ppm is assigned to different trigonal boron species distributed as boroxol and non-ring BO_3 units. While the more intensive and sharper peak located around 0 ppm is due to resonance of four-coordinate boron species.

It worthy to note that features of ^{11}BNMR spectra of cerium borate glasses [10] are quite different from that of—alkali and alkaline earth binary borate

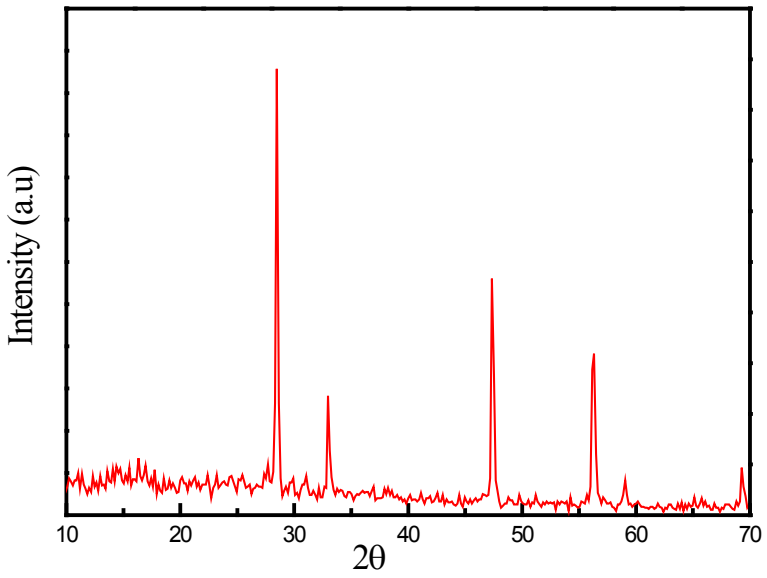

Figure 2. XRD patterns of pure CeO_2.

glasses. In glasses modified by CeO_2, the BO_4 and BO_3 peaks are being broader and totally overlapped, as presented in Figure 3. This was especially true for the glass containing 40 mol% CeO_2 which displayed asymmetrically broadened peak. The more pronounce broadening leads one to strongly suggest that presence of a BO_4 site with $2BO_3$ and $2CeO_4$ in next nearest neighbor environments. The difference in bond length and bond angle between B_3-O-Ce_4 and Ce_4-O-B_4 linkages is considered as the main reason for spectral broadening in glass containing 40 mol% CeO_2. On the other hand, glass containing 50 mol% CeO_2 showed more symmetric and less broadening behavior than that of glass containing 40 mol% CeO_2. This can be discussed on the bases of presence a BO_4 site coordinated with more CeO_4 units in next nearest neighbor environment. In this regard, BO_4 site with three or four CeO_4 sites may efficiently be formed. Enhancement of CeO_4 species around central B atom will result in increasing the symmetry elements in the whole glass network, since the majority of bonds are of Ce_4-O-Ce_4 type and limited bonds are formed with borate units. The symmetric of bonds around boron units will consequently change the value of chemical shift to become nearer to BO_4 surrounding with $4BO_3$, since the observed chemical shift is appeared around 0 ppm. In such a case, we can suggest that, chemical shielding of BO_4 coordinated with $4BO_3$ is similar to BO_4 coordinated with $4CeO_4$, since both possess the same value of chemical shift.

As shown in Figure 3, the lower value of CeO_2 (30 mol%) will affect the spectral feature, since two distinguished peaks are resolved. One characterizing BO_3 units and the other can be argued to be due to BO_4 site with $3BO_3$ and one CeO_4 sites. Presence of CeO_4 with lower site around BO_4 results in changing the

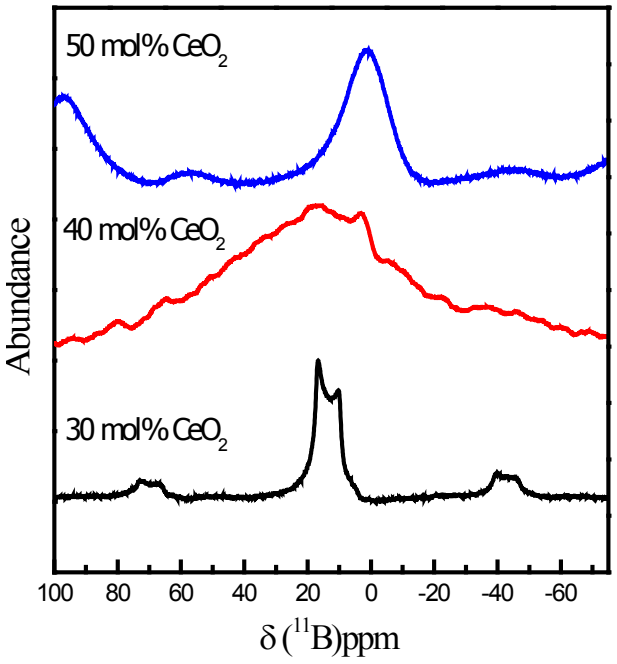

Figure 3. ^{11}B NMR spectra of binary cerium borate glasses as function of CeO_2 concentration.

position of spectral peak to more positive value since shielding of BO_4 atoms from BO_3 sites differs from that with CeO_4. Thus, chemical shifts of the studied system have obviously been varied from 12 ppm for glass containing 30 mol% CeO_2 to 0 ppm in glass enriched with CeO_2.

3.3. FTIR Analysis

FT-IR spectra of samples with x = 30, 40, 50 mol% CeO_2 are displayed in **Figure 4**. Three fundamental absorption bands [23] [30] [31] [32] have been observed in the borate glass system. The first band located between 600 - 800 cm^{-1} is assigned to symmetric bending vibrations of BO_3 bonds. The second band from 800 - 1200 cm^{-1} can be attributed to BO_4 stretching vibrations, while the third band from 1200 - 1600 cm^{-1} is assigned to B-O stretching vibrations of triangular BO_3 units.

As noted from **Figure 4**, structural changes appeared in a wide and asymmetric broadening, with increasing CeO_2 content. Particularly, these changes are notable in the intensity of band ranged between 800 to 1200 cm^{-1}. Such tendency is possible to the main role played by CeO_2 through presenting more CeO_4 units in the glass structure and their abilities to shield and coordinate with BO_4 units. As a consequence, increasing of CeO_2 at the expense of B_2O_3 results in increasing of Ce_4-O-Ce_4 bonds at expense of B_4-O-B_3. In such a case, the glass structure is mainly consisting of Ce_4-O bond in CeO_4 groups. Moreover, formation of some mixed vibrations from Ce_4-O with B_4-O and B_3-O may also be suggested. The results of these measurements are quite in good agreement with those obtained from NMR of the same glasses.

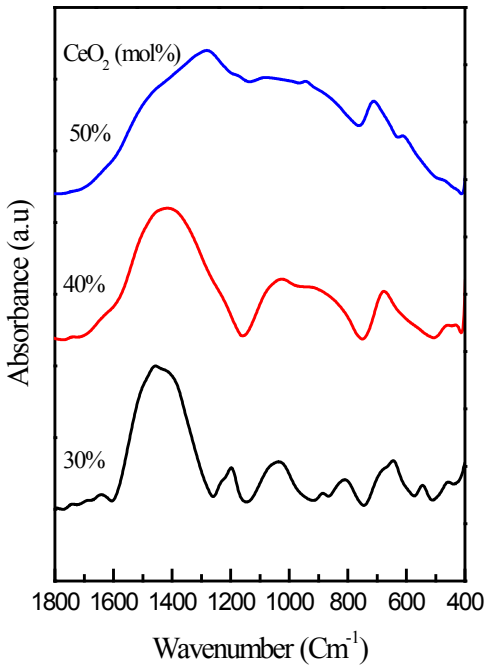

Figure 4. FTIR absorbance spectra of binary cerium borate glasses a function of CeO_2 concentration.

The total fraction of four-coordinated units, B_4, could be calculated for the three samples using a deconvolution procedure [5] [25] [31] [32]. This can be done by obtaining the relative area of each band corresponding to the structural units of both triangular BO_3 and tetrahedral BO_4 & CeO_4 units.

As a result, the value of B_4 is then defined as the ratio of the area related to the sum of structural groups containing BO_4 and CeO_4 four coordinated units to the area related to total units (BO_3 + BO_4 + CeO_4). Figure 5 represents an example for the deconvolution in Gaussian band of $50CeO_2{\cdot}50B_2O_3$ glass sample.

Figure 6 illustrates the change in the total fraction B_4 versus CeO_2 content of

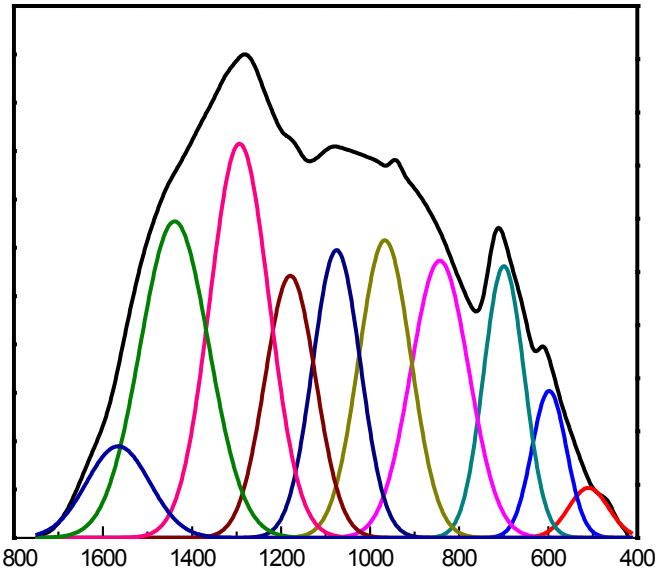

Figure 5. Deconvolution of infrared spectrum of the composition $50CeO_2{\cdot}50B_2O_3$ as an example for the analysis.

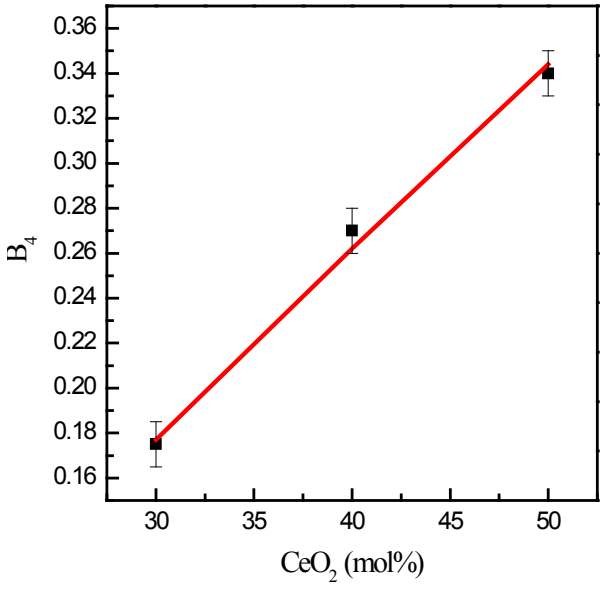

Figure 6. B_4 fraction of binary cerium borate glasses as function of CeO_2 concentration.

the studied glass samples. It can be observed from this figure, there is a linear dependence between B_4 and the change of CeO_2 composition. The role of CeO_2 in increasing B_4 may be attributed to the considerable frequent increasing in tetrahedral units in glass network at expense of BO_3 units. This reveals that the former role of cerium may become more dominant in glass riches with cerium oxide (50 mol%). In such a case, the linkage between CeO_4 and both BO_3 and BO_4 groups is being the most abundant within glass network. Such argument becomes clearly visible from FTIR spectra, particularly in glass of 50 mol% CeO_2, where the shoulder at about 1600 cm^{-1} is assigned to Ce-O vibration in phase rich with cerium borate mixed units.

4. Conclusions

The structural features of cerium borate glasses correlated with CeO_2 role have been investigated via different tools. The following conclusions can summarize the observed new features.

- XRD results revealed that, crystallization would take place in glasses with 50 mol% CeO_2. In such a glass, the principal crystalline phase is assigned to crystalline CeO_4, $CeBO_3$ and $Ce(BO_2)_3$ species which is mainly referred to both CeO_4 and BO_4 as dominated units.
- FTIR spectroscopy and NMR spectroscopy have confirmed that CeO_2 in binary borate glasses plays mainly the role of glass former in the form of CeO_4 units. The formation of expected ordered Ce_4-B-Ce_4 linkage impairs the conversion of triangular BO_3 units into BO_4 tetrahedra and causes a wide broadening in the spectrum.
- Increasing of the total fraction of all four coordinated units (B_4) is highly associated with increasing in CeO_4 concentration and this would consequently result in formation of more ordered structures.
- The change in chemical shifts of ^{11}B nuclei from 12 ppm to 0 ppm with increasing CeO_2 content from 30 to 50 mol% is considered due to formation of more shielded borate units via B-O-Ce bonds. Each born atom can be coordinated with 3 or 4 Ce atoms in the second coordination sphere.

References

[1] Pye, L., Fréchette, V. and Kreidl, N. (2012) Borate Glasses: Structure, Properties, Applications. Volume 12, Springer Science & Business Media, Part of the Materials Science Research Book Series, MSR.

[2] Bengisu, M. (2016) Borate Glasses for Scientific and Industrial Applications: A Review. *Journal of Materials Science*, **51**, 2199-2242.

[3] Oprea, I. (2005) Optical Properties of Borate Glass-Ceramics. PhD Diss., Osnabruck University, Germany.

[4] Minakova, N., Zaichuk, A. and Belyi, Y. (2008) The Structure of Borate Glass. *Glass and Ceramics*, **65**, 70-73.

[5] El-Damrawi, G. and El-Egili, K. (2001) Characterization of Novel CeO_2-B_2O_3 Glasses, Structure and Properties. *Physica B, Condensed Matter*, **299**, 180-186.

[6] Singh, G., Kaur, P., Kaur, S. and Singh, D. (2012) Investigation of Structural, Physical and Optical Properties of CeO_2-Bi_2O_3-B_2O_3 Glasses. *Physica B*: *Condensed Matter*, **407**, 4168-4172.

[7] Kelly, T., Petrosky, J., McClory, J., Adamiv, V., Burak, Y., Padlyak, B., Teslyuk, I., Lu, N., Wang, L., Mei, W. and Dowben, P. (2014) Rare Earth Dopant (Nd, Gd, Dy, and Er) Hybridization in Lithium Tetraborate. *Frontiers in Physics*, **2**, 31.

[8] Pisarski, W., Pisarska, J., Lisiecki, R., Dominiak-Dzik, G. and Ryba-Romanowski, W. (2010) Laser Spectroscopy of Rare Earth Ions in Lead Borate Glasses and Transparent Glass-Ceramics. *Laser Physics*, **20**, 649-655.

[9] Mansour, E., El-Egili, K. and El-Damrawi, G. (2007) Mechanism of Hopping Conduction in New CeO_2-B_2O_3 Semiconducting Glasses. *Physica B*: *Condensed Matter*, **389**, 355-361.

[10] El-Damrawi, G., Gharghar, F., Ramadan, R. and Aboelez, M. (2016) ^{11}B NMR Spectroscopy of Lead Borate Glasses: Additive Effect of Cerium Oxide. *New Journal of Glass and Ceramics*, **6**, 57.

[11] Trégouët, H., Caurant, D., Majérus, O., Charpentier, T., Cormier, L. and Pytalev, D. (2014) Spectroscopic Investigation and Crystallization Study of Rare Earth Metaborate Glasses. *Procedia Materials Science*, **7**, 131-137. https://doi.org/10.1016/j.mspro.2014.10.018

[12] Mansour, E., El-Egili, K. and El-Damrawi, G. (2007) Ionic-Polaronic Behavior in CeO_2-PbO-B_2O_3 Glasses. *Physica B*: *Condensed Matter*, **392**, 221-228. https://doi.org/10.1016/j.physb.2006.11.022

[13] Liu, H., Huang, J., Zhao, D., Yang, H. and Zhang, T. (2016) Improving the Electrical Property of CeO_2-Containing Sealing Glass-Ceramics for Solid Oxide Fuel Cell Applications: Effect of HfO_2. *Journal of the European Ceramic Society*, **36**, 917-923. https://doi.org/10.1016/j.jeurceramsoc.2015.10.004

[14] Zu, C., Chen, J., Zhao, H., Han, B., Liu, Y. and Wang, Y. (2009) Effect of Cerium on Luminescence and Irradiation Resistance of Tb^{3+} Doped Silicate Glasses. *Journal of Alloys and Compounds*, **479**, 294-298. https://doi.org/10.1016/j.jallcom.2008.12.037

[15] Girija, D., Naik, H., Sudhamani, C. and Kumar, B. (2011) Cerium Oxide Nanoparticles—A Green, Reusable, and Highly Efficient Heterogeneous Catalyst for the Synthesis of Polyhydroquinolines under Solvent-Free Conditions. *Archives of Applied Science Research*, **3**, 373-382.

[16] Culea, E., Neumann, M., Takacs, A., Pop, L., Culea, M., Bosca, M. and Marcean, R. (2005) Structural and Magnetic Behavior of Some Oxide Glasses Containing Cerium Ions. *Annals of the West University of Timisoara*, *Physics Series*, **46**, 117-120.

[17] Deshpande, V. and Taikar, R. (2010) Effect of Cerium Oxide Addition on Electrical and Physical Properties of Alkali Borosilicate Glasses. *Materials Science and Engineering*, **172**, 6-8. https://doi.org/10.1016/j.mseb.2010.04.003

[18] Jha, A. (2014) Rare Earth Materials: Properties and Applications. CRC Press, Boca Raton. https://doi.org/10.1201/b17045

[19] Kielty, M. (2016) Cerium Doped Glasses: Search for a New Scintillator. PhD, Clemson University, Clemson.

[20] Mansour, E., Doweidar, H., El-Damrawi, G. and Moustafa, Y. (2004) Mixed Alkali Effect in Polaronic Conducting Iron Borate Glasses. *Journal of Materials Science*, **39**, 4325-4329. https://doi.org/10.1023/B:JMSC.0000033418.94760.70

[21] Doweidar, H., Moustafa, Y., Abd El-Maksoud, S. and Silim, H. (2001) Properties of Na_2O-Al_2O_3-B_2O_3 Glasses. *Materials Science and Engineering*, **301**, 207-212.

https://doi.org/10.1016/S0921-5093(00)01786-X

[22] Doweidar, H., El-Damrawi, G. and Al-Zaibani, M. (2013) Distribution of Species in Na_2O-CaO-B_2O_3 Glasses as Probed by FTIR. *Vibrational Spectroscopy*, **68**, 91-95. https://doi.org/10.1016/j.vibspec.2013.05.015

[23] Gautam, C., Yadav, A. and Singh, A. (2012) A Review on Infrared Spectroscopy of Borate Glasses with Effects of Different Additives.

[24] Othman, H., Elkholy, H. and Hager, I. (2016) FTIR of Binary Lead Borate Glass: Structural Investigation. *Journal of Molecular Structure*, **1106**, 286-290. https://doi.org/10.1016/j.molstruc.2015.10.076

[25] El-Damrawi, G., Gharghar, F. and Ramadan, R. (2016) Structural Studies on New $xCeO_2 \cdot (50-x)PbO \cdot 50B_2O_3$ Glasses and Glass Ceramics. *Journal of Non-Crystalline Solid*, **452**, 291-296. https://doi.org/10.1016/j.jnoncrysol.2016.09.011

[26] Zhou, B., Sun, Z., Yao, Y. and Pan, Y. (2012) Correlations between ^{11}B NMR Parameters and Structural Characters in Borate and Borosilicate Minerals Investigated by High-Resolution MAS NMR and ab initio Calculations. *Physics and Chemistry of Minerals*, **39**, 363-372. https://doi.org/10.1007/s00269-012-0482-3

[27] Michaelis, V., Aguiar, P. and Kroeker, S. (2007) Probing Alkali Coordination Environments in Alkali Borate Glasses by Multinuclear Magnetic Resonance. *Journal of Non-Crystalline Solids*, **353**, 2582-2590. https://doi.org/10.1016/j.jnoncrysol.2007.04.029

[28] Clarida, W., Berryman, J., Affatigato, M., Feller, S., Kroeker, S., Zwanziger, W., Meyer, B., Borsa, F. and Martin, S. (2003) Dependence of N_4 upon Alkali Modifier in Binary Borate Glasses. *Physics and Chemistry of Glasses*, **44**, 215-217.

[29] Takaishi, T., Jin, J., Uchino, T. and Yoko, T. (2000) Structural Study of PbO-B_2O_3 Glasses by X-Ray Diffraction and ^{11}B MAS NMR Techniques. *Journal of the American Ceramic Society*, **83**, 2543-2548. https://doi.org/10.1111/j.1151-2916.2000.tb01588.x

[30] Ibrahim, S., Gomaa, M. and Darwish, H.H. (2014) Influence of Fe_2O_3 on the Physical, Structural and Electrical Properties of Sodium Lead Borate Glasses. *Journal of Advanced Ceramics*, **3**, 155-164. https://doi.org/10.1007/s40145-014-0107-z

[31] Verhoef, A. and Den Hartog, H. (1995) Infrared Spectroscopy of Network and Cation Dynamics in Binary and Mixed Alkali Borate Glasses. *Journal of Non-Crystalline Solids*, **182**, 221-234. https://doi.org/10.1016/0022-3093(94)00555-9

[32] Kamitsos, E., Patsis, A., Karakassides, M. and Chryssikos, G. (1990) Infrared Reflectance Spectra of Lithium Borate Glasses. *Journal of Non-Crystalline Solids*, **126**, 52-67. https://doi.org/10.1016/0022-3093(90)91023-K